



Title	Quantitative Detection and Fixation of Single and Multiple Gold Nanoparticles on a Microfluidic Chip by Thermal Lens Microscope
Author(s)	MAWATARI, Kazuma; TOKESHI, Manabu; KITAMORI, Takehiko
Citation	Analytical Sciences, 22(5), 781-784 https://doi.org/10.2116/analsci.22.781
Issue Date	2006-05-10
Doc URL	http://hdl.handle.net/2115/71669
Type	article
File Information	Anal.sci.22-781.pdf



[Instructions for use](#)

Quantitative Detection and Fixation of Single and Multiple Gold Nanoparticles on a Microfluidic Chip by Thermal Lens Microscope

Kazuma MAWATARI,* Manabu TOKESHI,** and Takehiko KITAMORI*.,***.***†

**Microchemistry Group, Kanagawa Academy of Science and Technology (KAST), KSP East 307, 3-2-1 Sakado, Takatsu, Kawasaki, Kanagawa 213-0012, Japan*

***Institute of Microchemical Technology (IMT), KSP East 207, 3-2-1 Sakado, Takatsu, Kawasaki, Kanagawa 213-0012, Japan*

****Department of Applied Chemistry, School of Engineering, The University of Tokyo, 7-3-1 Hongo, Bunkyo, Tokyo 113-8656, Japan*

A detection and fixation method of single and multiple gold nanoparticles on the wall of a microfluidic channel is demonstrated. A thermal lens microscope (TLM) with continuous-wave excitation (wavelength, 532 nm) and probe (wavelength, 670 nm) laser beams was used to realize the sensitive detection of heat generated by light absorption of individual gold nanoparticles (50 nm in diameter); fixation of the individual nanoparticles was realized simultaneously. The fixation mechanism was investigated and attributed to an absorption-based optical force. In addition to single nanoparticle detection, multiple-nanoparticle detection and fixation was demonstrated. An acceleration of fixation was observed when the number of fixed particles was increased. TLM is expected to be a powerful tool for both the quantitative detection and precise fixation of individual nanoparticles.

(Received December 12, 2005; Accepted February 20, 2006)

Introduction

Nanoparticles are now gaining much attention due to their unique physical and chemical properties, and are becoming recognized as one of the key materials in nanoscience and nanotechnology. Especially, gold nanoparticles are widely used for such activities as surface-enhanced Raman scattering (SERS),^{1,2} catalysis,³ labels for biomolecules detection^{4,5} and nonlinear optical materials.⁶ The unique properties arise from the surface plasmon band, and are due to their nanometer scale size. In addition, these properties are known to change with their size, shape, aggregation, surface morphology and the environment.⁷

Nanoparticles have mainly been used either as substrates for sensitivity enhancement by a strong electric field (SPR, luminescence, SERS, etc.) or as stable and universal labels for biomolecule detection utilizing immunoassay or other specific reactions on a solid surface. Recently, single-nanoparticle chemical sensors have been reported.^{8,9} The merits of single-nanoparticle sensors include reduced sample amount and high sensitivity due to the narrow line width of a single nanoparticle spectrum. Also, single nanoparticle sensors are expected to be applied to the array format for high-throughput analysis, due to its small size. Therefore, both the quantitative detection and fixation methods of individual nanoparticles in a controllable way are important for nanoparticles-based analytical applications.

So far, self-assembly and surface modification methods have been used for fixation and pattern formation of nanoparticles on substrates.¹⁰ However, these methods have been used to treat many particles simultaneously, though the control of individual nanoparticles was difficult. Therefore, fixation methods that are capable of controlling the position and the number of nanoparticles are desired for fixing of individual nanoparticles. Furthermore, the utilization of a microfluidic chip ensures the full potential of a single nanoparticle-based sensor due to the reduced sample volume and high reaction efficiency due to the large surface-to-volume ratio.

Recently, new physical fixation methods have been developed that utilize the light energy of an ultraviolet (UV) laser or a visible pulsed laser with a few nanoseconds pulses.^{11,12} For example, the fixation of gold nanoparticles in a fused-silica capillary (i.d. 50 μm) was reported for spatioselective electroless plating by a 532 nm pulsed laser.¹³ Furthermore, the fixation of single gold nanoparticles of 80 nm in diameter was achieved by focusing a 355 nm pulsed laser beam.¹¹ With the focused laser beam, the positions of the fixed nanoparticles were expected to be controlled with micro-scale precision.

However, a quantitative detection method of individual nanoparticles in liquid was not achieved due to a difficulty of detection on a nanometer scale region in the liquid. Laser-assisted adsorption is a stochastic process,¹¹ and a simultaneous quantitative detection and fixation method is necessary for accurate control of the number of fixed nanoparticles and the position at the single nanoparticle level. In addition to the single nanoparticle fixation, the fixation of multiple gold nanoparticles is important for enhancing the surface electric

† To whom correspondence should be addressed.
E-mail: kitamori@icl.t.u-tokyo.ac.jp

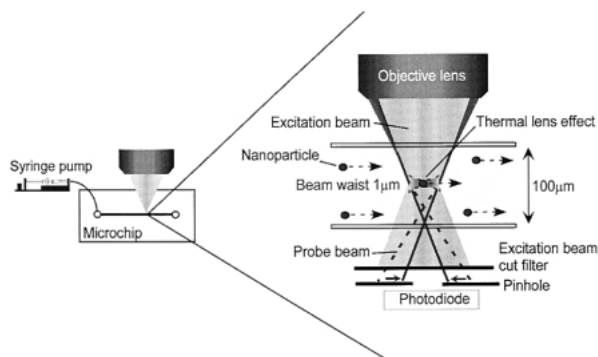


Fig. 1 Principle of the detection of individual nanoparticles by TLM.

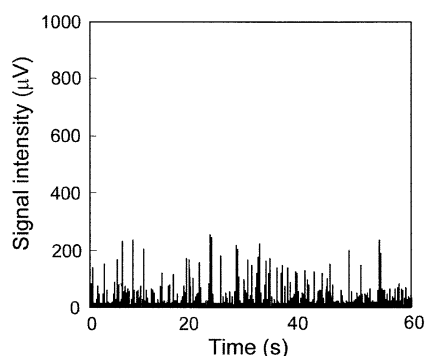


Fig. 2 Waveform of counting individual gold nanoparticles of 50 nm diameter (number density: 3×10^{10} particles/L) by focusing the excitation laser beam in the center of the microfluidic channel. The time constant was set at 1 ms.

field (*e.g.* SPR, luminescence, SERS).

Thermal lens spectrometry (TLM) is a promising method for the sensitive detection of non-fluorescent samples.¹⁴⁻¹⁷ We have developed a thermal lens microscope (TLM) for sensitive detection in a microspace.^{18,19} In TLM, an excitation laser beam is focused into the sample by an objective lens with a high numerical aperture. The sample absorbs the excitation laser beam and releases the light energy as thermal energy, following non-radiative relaxation. Then, a probe laser beam detects the temperature distribution as a thermal-lens effect. The detection limit was proved to be as low as the 0.1 nM level, which corresponded to a sub-single molecule in a 7 fL detection volume.²⁰ Taking advantage of the high sensitivity and wide applicability, we successfully applied TLM to various analytical fields, such as immunoassay,²¹ environmental analysis²² and single-cell analysis²³ on microfluidic chips. In a previous report, we found that TLM could detect individual Ag nanoparticles (10 nm in diameter) in solution by a single nanoparticle photothermal effect.²⁴

In this report, we demonstrate both the quantitative detection and fixation of single and multiple gold nanoparticles (50 nm in diameter) in a microfluidic glass chip. TLM with continuous-wave (CW) excitation and probe laser beams was utilized. Single and multiple nanoparticles were quantitatively detected and fixed on a bare glass surface under flow conditions for the first time. The process of single and multiple nanoparticles fixation was investigated. The capability of TLM was verified for both the detection and fixation of single and multiple gold nanoparticles.

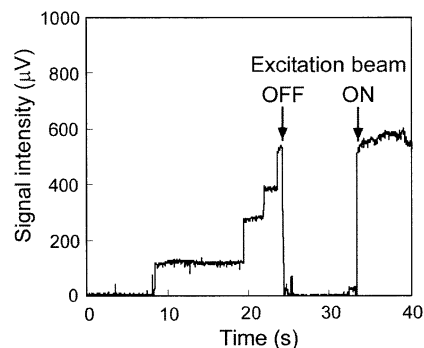


Fig. 3 Measurement of a stepwise signal increase when the excitation laser beam was focused on the lower wall of the microfluidic channel.

Experimental

Colloidal gold solutions (particle diameter, 50 nm; coefficient of variance, < 20%) were used as samples (Funakoshi Co., Ltd.). The stock solutions were diluted with pure water before measurements. A straight-shaped microfluidic channel (250 μm wide \times 100 μm deep \times 60 mm long) was fabricated on a microchip made of fused silica (Mitorika Glass Co., Ltd.). Details of its fabrication procedure were reported previously.²⁵ The wall of the microfluidic channel was kept as a bare glass surface. The sample solutions were introduced into the microfluidic channel and driven by a syringe pump at 0.25 $\mu\text{L}/\text{min}$ (average velocity: 170 $\mu\text{m}/\text{s}$).

The TLM system was described previously.^{20,26} The principle of individual nanoparticle detection by TLM is illustrated in Fig. 1. The 532 nm CW laser beam was used as an excitation beam (20 mW at the sample; intensity modulated at 1.1 kHz) and a 670 nm CW laser beam was used as a probe beam (0.5 mW at the sample). These two beams were made coaxial and focused in the microfluidic channel by an objective lens (numerical aperture: 0.75). The spot size of the excitation beam was about 1 μm in diameter, and the power density was calculated to be 2.5 MW/cm^2 . In the microfluidic channel, a transient photothermal effect was induced due to absorption of the excitation beam by individual nanoparticles when they passed through the focus region. The resultant temperature distribution induced the refractive index distribution around the nanoparticles, which acted as an optical element to deflect the probe beam. The intensity change of the transmitted probe beam through a pinhole was detected by a photodiode and a lock-in amplifier (time constant of 3 ms, unless otherwise mentioned). The amplitude signal of the lock-in amplifier was used as a photothermal signal and recorded.

Results and Discussion

When the excitation laser beam is focused in the center of the microfluidic channel, the individual gold nanoparticles can be counted individually without fixation on the upper or lower wall of the channel. The counting waveform of the gold nanoparticles (number density of 3×10^{10} particles/L) in the center of the channel is shown in Fig. 2. The time constant was set at 1 ms. Clear pulsed signals were observed for irradiation of both the excitation and probe beams. The pulse count was confirmed to increase linearly with the number density of the

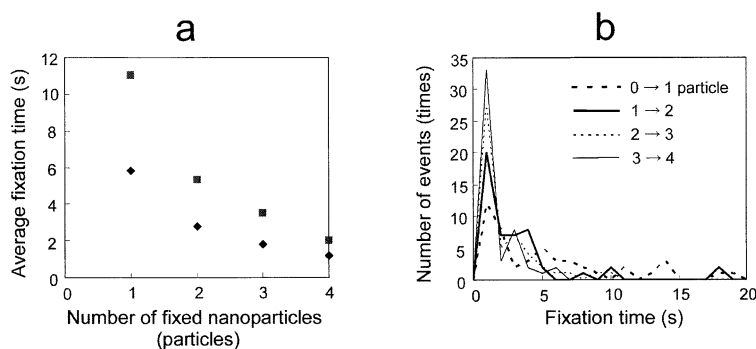


Fig. 4 Measurement of the fixation time for single and multiple gold nanoparticles. (a) Dependence of the average fixation time on the number of fixed gold nanoparticles (number density, 3×10^{10} particles/L for symbol (■) and 6×10^{10} particles/L for symbol (◆)). (b) Histogram (the number of events in 1 s interval was counted for a total of 50 events, and the number density was 6×10^{10} particles/L).

gold nanoparticles in the range of 10^{10} – 10^{12} particles/L, and was zero for water (blank). Therefore, each pulse corresponded to the photothermal signals of individual nanoparticles. The average pulse height was calculated to be $80 \mu\text{V}$.

On the other hand, when the excitation beam was focused on the lower wall of the channel, a stepwise increase of signal intensity was found, as shown in Fig. 3. The increase was observed with the irradiation of both the excitation beam and the probe beam, and it was not observed for pure water (blank). In addition, the expected value of the nanoparticles in the detection volume ($< 1 \text{ pL}$)²⁴ was calculated to be less than 0.03 particles. Therefore, the signals were attributed to the photothermal signals of individual gold nanoparticles. Moreover, the signal intensity was retained after turning off and on the excitation beam, as shown in Fig. 3. Then, the optical trapping effect by the focused excitation laser beam was ignored. As a result, the number of fixed nanoparticles could be controlled just by turning the excitation beam off at the timing corresponding to the desired number of fixed nanoparticles. The signal intensity decreased to zero by changing the focus position in the plane of the wall surface. After that, the stepwise signal increase was observed again. As a consequence, these stepwise increases were considered to be laser-assisted fixation of individual gold nanoparticles in the microfluidic glass channel.

We next investigated the mechanism of nanoparticle fixation. The number of events of a single nanoparticle fixation was measured by focusing laser beams on the upper and lower walls at different positions. The measurement time was 10 min for each position. No signals were observed when focusing the excitation beam on the upper wall. However, 51 pulse signals (events) were observed for focusing on the lower wall. Both the upper and lower walls were kept as bare glass surfaces. Therefore, some optical force was working to push the nanoparticles in the optical-axis direction. It was previously reported that 80 nm gold nanoparticles were trapped by a near-IR (1064 nm wavelength) focused laser beam with small optical absorption.¹¹ In our experiment, the excitation wavelength was almost the maximum of the absorption band of the gold nanoparticles. In addition, the diameter of the gold nanoparticles that we used was smaller. Therefore, optical absorption-based forces could have played a major role in the fixation process.

Finally, we measured the time distribution for the fixation of multiple nanoparticles by focusing the excitation laser beam on

the lower wall. The time intervals between stepwise increases were measured from one nanoparticle to four nanoparticles fixation in 50 waveforms. The result is as shown in Fig. 4. As expected, the average fixation time decreased by increasing the number density of the sample solutions (Fig. 4a). However, a decrease of the average fixation time was observed with an increase of the number of fixed nanoparticles. Assuming that the multiple fixation process occurred independently with the number of fixed nanoparticles, we would expect the average fixation time to be almost the same. Then, the decrease of the time might be attributed to the existence of attractive forces between the nanoparticles. In addition, it was reported that aggregation of the gold nanoparticles was accelerated by irradiating the visible laser at the wavelength of the surface plasmon absorption.²⁷

The power density of the excitation beam was 2.5 MW/cm^2 . This value was below the reported threshold of the fragmentation (about 13 MW/cm^2 , calculated from 80 mJ/cm^2 in the literature),¹¹ though the present experimental conditions (smaller diameter of nanoparticles and longer laser beam wavelength) are different. The exact shape of the fixed nanoparticles is under investigation.

Conclusions

We quantitatively detected and controlled the number of fixed gold nanoparticles on the wall of the microfluidic glass channel. A difference in the fixation mechanism was observed between single and multiple fixation processes. The spatial resolution was estimated to be less than $1 \mu\text{m}$ based on the spot size of the excitation beam. Accurate control of the fixation was achieved through simultaneous detection and fixation by sensitive TLM. For future applications, the gold nanoparticles can be modified to provide various surface chemistries, and an array of single nanoparticles with different surface molecules for recognition of sample is achieved by changing the reagents, followed by fixation at a determined position. For SERS measurements, multiple gold nanoparticles can be prepared after sample adsorption. In addition to arrayed substrate production, TLM will be used for detecting the interaction of single biomolecules by labeling them with gold nanoparticles. Therefore, this method using a microfluidic channel is expected to become a valuable tool for high-throughput and highly sensitive nanoparticle-based sensors.

Acknowledgements

We acknowledge Dr. Akihito Hibara of The University of Tokyo for useful discussions and suggestions.

References

1. D. S. Grubisha, R. J. Lipert, H. Y. Park, J. Driskell, and M. D. Porter, *Anal. Chem.*, **2003**, *75*, 5936.
2. J. Jiang, K. Bosnick, M. Maillard, and L. Brus, *J. Phys. Chem. B*, **2003**, *107*, 9964.
3. B. L. V. Prasad, S. I. Stoeva, C. M. Sorensen, V. Zaikovski, and K. J. Klabunde, *J. Am. Chem. Soc.*, **2003**, *125*, 10488.
4. R. C. Bailey, J. M. Nam, C. A. Mirkin, and J. T. Hupp, *J. Am. Chem. Soc.*, **2003**, *125*, 13541.
5. K. Sato, K. Hosokawa, and M. Maeda, *J. Am. Chem. Soc.*, **2003**, *125*, 8102.
6. C. P. Collier, R. J. Saykally, J. J. Shiang, S. E. Henrichs, and J. R. Heath, *Science*, **1997**, *277*, 5334.
7. S. Link and M. A. El-Sayed, *J. Phys. Chem. B*, **1999**, *103*, 8410.
8. G. Raschke, S. Kowarik, T. Franzl, C. Sonnichsen, T. A. Klar, J. Feldmann, A. Nichtl, and K. Kurzinger, *Nano Lett.*, **2003**, *3*, 935.
9. G. Raschke, S. Brogl, A. S. Susa, A. L. Rogach, T. A. Klar, J. Feldmann, B. Fieres, N. Petkov, T. Bein, A. Nichtl, and K. Kurzinger, *Nano Lett.*, **2004**, *4*, 1853.
10. W. X. Zheng, M. M. Maye, F. L. Leibowitz, and C. J. Zhong, *Anal. Chem.*, **2000**, *72*, 2190.
11. S. Ito, H. Yoshikawa, and H. Masuhara, *Appl. Phys. Lett.*, **2002**, *80*, 482.
12. Y. Niidome, A. Hori, H. Takahashi, Y. Goto, and S. Yamada, *Nano Lett.*, **2002**, *1*, 365.
13. Y. Niidome, H. Takahashi, T. Kawasaki, A. Hori, and S. Yamada, *Jpn. J. Appl. Phys.*, **2003**, *42*, 7640.
14. N. J. Dovichi and J. M. Harris, *Anal. Chem.*, **1979**, *51*, 728.
15. N. J. Dovichi and J. M. Harris, *Anal. Chem.*, **1980**, *52*, 2338.
16. N. J. Dovichi and J. M. Harris, *Anal. Chem.*, **1980**, *52*, 695A.
17. N. J. Dovichi and J. M. Harris, *Anal. Chem.*, **1981**, *53*, 689.
18. K. Uchiyama, A. Hibara, H. Kimura, T. Sawada, and T. Kitamori, *Jpn. J. Appl. Phys.*, **2000**, *39*, 5316.
19. T. Kitamori, M. Tokeshi, A. Hibara, and K. Sato, *Anal. Chem.*, **2004**, *76*, 52A.
20. M. Tokeshi, M. Uchida, A. Hibara, T. Sawada, and T. Kitamori, *Anal. Chem.*, **2001**, *73*, 2112.
21. K. Sato, M. Tokeshi, T. Odake, H. Kimura, T. Ooi, M. Nakao, and T. Kitamori, *Anal. Chem.*, **2000**, *72*, 1144.
22. M. Tokeshi, T. Minagawa, K. Uchiyama, A. Hibara, K. Sato, H. Hisamoto, and T. Kitamori, *Anal. Chem.*, **2002**, *74*, 1565.
23. E. Tamaki, K. Sato, M. Tokeshi, K. Sato, M. Aihara, and T. Kitamori, *Anal. Chem.*, **2002**, *74*, 1560.
24. K. Mawatari, T. Kitamori, and T. Sawada, *Anal. Chem.*, **1998**, *70*, 5037.
25. K. Sato, M. Tokeshi, T. Kitamori, and T. Sawada, *Anal. Sci.*, **1999**, *15*, 647.
26. S. Hiki, M. Tokeshi, A. Hibara, and T. Kitamori, *Bunseki Kagaku*, **2003**, *52*, 569.
27. H. Eckstein and U. Z. Kreibig, *Phys. D*, **1993**, *26*, 239.